

Cooperative Detection for mmWave Radar-Communication Systems

Christodoulos Skouroumounis, Constantinos Psomas, and Ioannis Krikidis

IRIDA Research Centre for Communication Technologies,

Department of Electrical and Computer Engineering, University of Cyprus, Cyprus

Email: {cskour03, psomas, krikidis}@ucy.ac.cy

Abstract—Spectral co-existence of radar and communication (RadCom) systems causes mutual interference between the two systems, compromising both the data exchange and radar sensing capabilities. Focusing on the radars' detection performance, in this paper, we propose a novel cooperative detection technique in the context of millimeter-wave (mmWave) RadCom systems, under a constant false alarm constraint. Existing detection techniques assign a single base station (BS) operating in radar mode (RM) for the detection of a target. In contrast, our proposed technique performs joint target detection through multiple cooperative RM-enabled BSs (RBSs). Specifically, our proposed technique exploits the fusion of individual sensing information by a set of pre-selected cooperative RBSs, aiming at enhancing the detection performance. We consider three pre-selection policies based on: 1) the Euclidean distance, 2) the received signal power, and 3) a random selection. In addition, for the fusion of the sensing information, we consider three hard-decision combining rules, namely *OR*, *Majority* and *AND* rule. By using stochastic geometry tools, analytical expressions for the detection performance are expressed for each pre-selection policy and combining rule. Our results reveal that the proposed technique significantly improves the detection performance of the mmWave RadCom systems.

Index Terms—Radars, millimeter-wave, cooperative target detection, stochastic geometry.

I. INTRODUCTION

Emerging applications such as smart cars, unmanned aerial vehicles (UAV) and enhanced localization, lead to an ever-increasing demand for systems with both communication and radar sensing capabilities [1]. In order to address this demand, joint communication and radar sensing techniques have been developed, integrating the two operations of communication and radar sensing over a shared spectrum. As an emerging research topic, the spectrum sharing of radar and communication (RadCom) systems enables the efficient use of the available spectrum, providing a new way for designing and modeling novel network architectures and protocols that can benefit from the synergy of RadCom systems.

As a straightforward approach for achieving the spectral co-existence of RadCom systems, the authors in [2] consider an opportunistic spectrum sharing scheme between a pulsed radar device and a cellular network, where the communication system transmits if and only if its transmission will not compromise the operation of the radar system. While such approach achieves low implementation complexity, the simultaneous operation of communication and radar sensing systems

is unattainable. The main challenge for the joint operation of RadCom systems over a shared spectrum is the negative effects of the mutual interference between the two systems. The impact of mutual interference on the coverage performance of communication systems is well investigated in the literature, however, its impact on the sensing capabilities of radar systems has not fully elucidated. The concept of radar sensing refers to the use of radio signals in order to retrieve short-range environmental information through measuring various parameters, such as an object's location, moving speed, and shape [1]. The work in [3] considers the trade-off emerging in networks, where the terminals switch between radar mode (RM) for target detection and communication mode (CM) for data exchange, sharing the same bandwidth. This work is further extended in [4], where the authors quantify the effect of mutual interference on the radar detection and the communication network throughput.

The requirements of next generation cellular networks in massive connectivity and high throughput, motivate their operation in millimeter-wave (mmWave) frequency bands. MmWave communications are considered as a suitable environment for integrating RadCom systems due to their unique features [1]. In particular, the large available bandwidth of mmWave communications can lead to multi-Gbps rates, which is essential to satisfy the high-capacity requirements of emerging applications in RadCom systems. Furthermore, the higher path-losses of the mmWave signals and their sensitivity to blockages, can improve the network performance by mitigating the overall interference [5]. Therefore, the modeling and the analysis of RadCom systems in mmWave frequency band, is of critical importance in order to support the massive data-rate demands of emerging applications and combat the severe multi-user interference. The authors in [6] investigate the implementation of RM-enabled mmWave base stations (BSs) in the context of vehicular systems, and study the impact of the radar interference on the detection performance. Finally, the authors in [7] characterize the blockage detection probability achieved by the mmWave RM-enabled BSs (RBSs), and provide guidelines for the efficient deployment of the BSs. Nevertheless, the exploitation of radar cooperation aiming to mitigate the overall interference and enhance the target detection in the context of mmWave RadCom systems is missing from the literature.

In this paper, we evaluate the impact of BS cooperation on the detection performance of mmWave RadCom systems, where the network's nodes can operate either in CM or RM. The main contribution is the development of a novel cooperative multi-point detection (CoMD) technique, aiming the

This work was supported by the Research Promotion Foundation, Cyprus, under the projects INFRASTRUCTURES/1216/0017 (IRIDA) and EXCELLENCE/0918/0377 (PRIME). This work was also supported by the European Research Council (ERC) under the European Union's Horizon 2020 research and innovation programme (Grant agreement No. 819819).

enhancement of the detection performance. In particular, our proposed technique exploits the fusion of individual sensing informations by a set of pre-selected RBSs, in order to elevate the network's detection capability. We evaluate the achieved performance in the context of two popular and well investigated selection policies, which are based on the Euclidean distance and the received signal power. For comparison purposes, we also investigate our proposed technique with a random RBS selection policy. For the fusion of individual sensing information by the cooperative RBSs, three hard-decision fusion rules, *OR*, *Majority* and *AND* rules, are analyzed. Based on the developed mathematical framework and by leveraging tools from stochastic geometry, analytical expressions are derived for the network's detection performance for each pre-selection policy and combining rule. Our results illustrate that our cooperative technique can significantly improve the detection performance of RadCom systems, when compared to the conventional non-cooperative radar detection technique. Finally, our results pinpoint the role of mmWave characteristics and spectrum sharing parameters, offering insights into how key parameters affect the performance.

Notation: $\binom{n}{k} = \frac{n!}{k!(n-k)!}$ is the binomial coefficient, $\Gamma[a]$ and $\Gamma[a, x]$ denote the complete and incomplete gamma function, respectively, and $\mathcal{G}[a, b]$ denotes a gamma random variable with shape parameter a and scale parameter b .

II. SYSTEM MODEL

A. Network topology

Consider a cellular network consisting of randomly located BSs that operate in the mmWave frequency band. The BSs are uniformly distributed in \mathbb{R}^2 according to an independent homogeneous Poisson Point Process (PPP) denoted as $\Phi = \{x_j \in \mathbb{R}^2, j \in \mathbb{N}^+\}$ with density λ , and transmit with power equal to P_t . We assume that all BSs are connected to a central unit, also known as fusion center (FC), through an ideal report channel [4]. In addition, we assume that each BS can operate either in RM or CM with probabilities ϱ and $1 - \varrho$, respectively, where $\varrho \in [0, 1]$. Hence, Φ can be partitioned into two independent and homogeneous PPPs i.e., Φ_r with density $\lambda_r = \lambda\varrho$ and Φ_c with density $\lambda_c = \lambda(1 - \varrho)$, such that $\Phi = \Phi_c \cup \Phi_r$. Particularly, the CM-enabled BSs (CBSs) serve their associated users in the downlink (DL) direction, while the RBSs are responsible for detecting a target. Without loss of generality and following Slivnyak's theorem, we study the detection performance of the typical target located at the origin.

All wireless signals are assumed to experience both large-scale path-loss effects and small-scale fading; the network is considered to be interference-limited. We assume that the small-scale fading between two BSs is modeled by Nakagami fading, where different links are assumed to be independent and identically distributed. Thus, the power of the channel fading is a normalized Gamma random variable with shape and scale parameters m and $1/m$, respectively i.e., $h \sim \mathcal{G}[m, 1/m]$. For the large-scale path-loss between BSs x and y , we assume an unbounded path-loss model, $L(x, y) = \|x - y\|^{-a}$, where $a > 2$ is the path-loss exponent.

B. Blockage and Sectorized antenna Model

We adopt a blockage model for modeling the susceptibility of mmWave signals to blockage effects. Specifically, a mmWave link can be either line-of-sight (LoS) or non-LoS (NLoS), depending on whether the transmitter is visible to the receiver or not, due to the existence of blockages. To simplify the mathematical derivation in the system-level analysis, we consider the generalized *LoS ball* model [8], where the LoS probability function can be approximated by a step function. Specifically, a link of length r is in LoS state with probability $p(r) = p_L \mathbb{1}(r \leq R)$, where $\mathbb{1}(X)$ is an indicator function of the event “ X is true”, R is the maximum length of an LoS link [8] and the constant $p_L \in [0, 1]$ represents the average fraction of the LoS area in the ball of radius R . In this paper, the interference effect from the NLoS signals is ignored, since the dominant interference is caused by the LoS signals [8].

For modeling the antenna directionality of BSs, we adopt an ideal cone antenna pattern. The antenna array gain is parameterized by two values: 1) main-lobe beamwidth $\phi \in [0, 2\pi]$, and 2) main-lobe gain G (dB). Regarding the communication operation, we assume that perfect beam alignment can be achieved for the link between each user and its serving CBS using the estimated angles of arrival. On the other hand, the beams of interfering links are assumed to be randomly oriented with respect to each other. It is important to mention that, an interfering BS causes interference to another BS, only if the alignment of their two randomly oriented antenna patterns overlap. Hence, the active interfering LoS BSs form a PPP $\Phi_{\mathcal{I}}$ of intensity $\lambda_{\mathcal{I}}(r) = \frac{\lambda\phi}{2\pi}p(r)$.

C. Radar Detection Model

Considering a time period of M time-slots, we assume that an RBS broadcasts a pilot sequence towards its main-lobe direction during the first time-slot. Over the subsequent time-slots i.e. $M - 1$, the RBS measures the reflected signal power received within its main-lobe direction. Based on the received signal power, an RBS determines whether an obstacle exists in the current direction. In the next M time-slots, the RBS changes the direction and repeats the same process. Focusing on a particular time-slot, the reflected signal power received by the RBS at u , is given by $\mathcal{S}_r = P_t G \frac{\sigma \ell}{4\pi} h r_u^{-2a}$ [4], where $r_u = \|u\|$, $h \sim \mathcal{G}[m, 1/m]$, σ is the cross-section area of the typical target; $\ell = c/(4\pi f)^2$, c is the speed of light and f is the carrier frequency. In addition to the reflected signal power, each RBS receives the aggregated interference caused by the nearby BSs, $v \in \Phi_{\mathcal{I}} \setminus u$, which lie in the main-lobe direction. Hence, the aggregate interference over time-slot τ , is given by

$$\mathcal{I}_{\tau} = \sum_{v \in \Phi_{\mathcal{I}} \setminus u} P_t G^2 \ell g \|v - u\|^{-a} \stackrel{(a)}{=} \sum_{v \in \Phi_{\mathcal{I}} \setminus u} P_t G^2 \ell g r_v^{-a}, \quad (1)$$

where (a) is based on Slivnyak's theorem and g denotes the channel power of an interfering link, i.e. $g \sim \mathcal{G}[m, 1/m]$.

In this paper, we assume that all RBSs implement a detection rule based on the received power, declaring a target to be present if the overall received power exceeds a detection threshold ϑ . In particular, the typical target is correctly detected from the RBS at u in time-slot τ , if $\mathcal{S}_r + \mathcal{I}_{\tau} \geq \vartheta$. Conversely, in

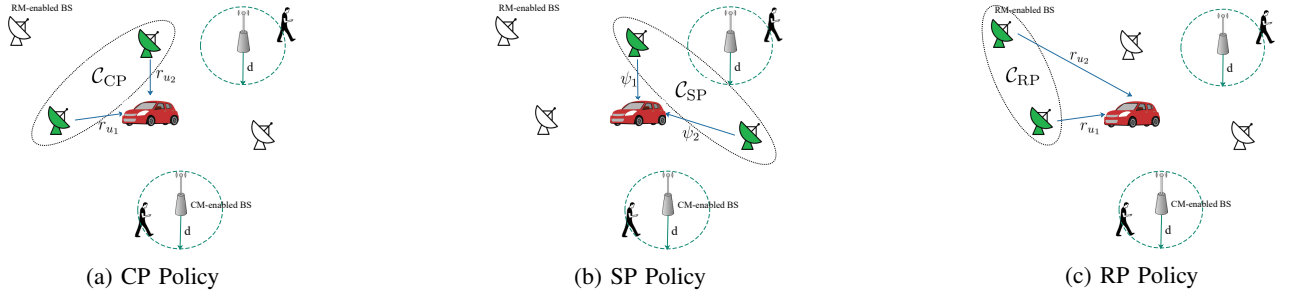


Fig. 1: The three considered pre-selection policies.

the case where the typical target is absent and the interference level observed by a RBS is strong enough to exceed the detection threshold, i.e. $\mathcal{I}_\tau \geq \vartheta$, a false alarm is triggered. In order to keep the probability of false alarm at a desirable level, in Section IV we set the detection threshold ϑ according to the observed interference.

D. Communication Model

Each CBS performs DL transmission to satisfy its associated user, which is randomly located in a circle of radius R centered at the CBS. We investigate the probability of a user to successfully decode a packet that is sent over time-slot τ , which is the probability that the signal-to-interference ratio (SIR) is greater than a threshold γ i.e., $\mathcal{P}_c = \mathbb{P}[\text{SIR} > \gamma]$. The received signal at the user from its serving CBS is given by $\mathcal{S}_c = P_t G^2 \ell h d^{-a}$. Regarding the observed interference, we assume that the interference caused by the neighboring targets due to the reflected radar signals is negligible and the dominant interference is caused by the BSs. The aforementioned probability is evaluated in the following Lemma, for the special case $m = 1$ and $a = 4$.

Lemma 1. A user, which is at distance d from its serving CBS, successfully decode at time-slot τ with probability

$$\mathcal{P}_c = \int_0^R 2\pi\lambda_r d e^{-\pi\lambda_r d^2 - \frac{\lambda}{2} d^2 \Delta \gamma^{\frac{1}{2}} \left(\text{arccot}(\gamma^{\frac{1}{2}}) - \arctan\left(\frac{R^2}{d^2 \gamma^{\frac{1}{2}}}\right) \right)} dd, \quad \text{where } \Delta = \phi p_L (M(1 - \varrho - 1) - \varrho) / M.$$

Remark 1. For low values of ϱ , \mathcal{P}_c increases, while for high values \mathcal{P}_c decreases.

The coverage probability is well-examined in the literature [4], and therefore, in the rest of this paper we focus on the detection performance of RadCom systems.

III. COOPERATIVE BS DETECTION TECHNIQUE

Within the considered network deployment, we focus on the impact of BS cooperation on the network's detection performance. Specifically, we propose a CoMD technique which is based on a two-level procedure. Initially, in the first-level phase, the set of cooperative RBSs is pre-selected, consisting of the η RBSs that satisfy the rules of the adopted pre-selection policy (see Section III-A). At the second-level phase, each cooperative RBS takes an independent binary (hard) decision on the typical target presence. Finally, based on the adopted hard-decision combining rule (see Section III-B), the FC processes the individual sensing information, providing the final

decision regarding whether the typical target is present or not. Fig. 1 schematically depicts the three considered pre-selection policies, where the colored nodes represent the η pre-selected RBSs that form the set of cooperative RBSs. Note that, the set of cooperative RBSs may consist of different pre-selected RBSs depending on the adopted pre-selection policy.

In the following sections, the three pre-selection policies are presented along with the set of cooperative RBSs for each policy and the three combining rules utilized at the FC are introduced.

A. Pre-selection Policies

1) *Closest LoS policy (CP)*: Firstly, we consider the case where the set of cooperative RBSs to detect their associated target, consists of the η closest LoS RBSs of the typical target. Fig. 1a schematically depicts the CP policy. The CP policy requires an a priori knowledge of the location of the RBSs, which can be obtained by monitoring the location of the RBSs through a low-rate feedback channel [5]. In this case, the set of η cooperative RBSs, is defined as

$$\mathcal{C}_{CP} = \left\{ u_i : u_i = \arg \max_{x \in \Phi_r \setminus \{u_1, \dots, u_{i-1}\}} \|x\|^{-1}, i \in \{1, \dots, \eta\} \right\}, \quad (2)$$

where u_i represents the location of the i -th closest LoS RBS. Let \mathbf{r}_u represents the vector consisting the distances from the η pre-selected RBSs, i.e. $\mathbf{r}_u = \{r_{u_1}, \dots, r_{u_\eta}\}$, where $i \in \{1, \dots, \eta\}$. The following proposition provides the joint probability density function (pdf) of the distances between the typical target and its η pre-selected RBSs.

Proposition 1. The joint pdf of the distances between the typical target and its η closest LoS RBSs, is given by

$$f_{\Phi_r}^{CP}(\mathbf{r}_u) = (2\pi\lambda_r)^\eta \exp(-\pi\lambda_r p_L r_{u_\eta}^2) \prod_{i=1}^\eta p(r_{u_i}) r_{u_i}. \quad (3)$$

Proof. The proof of Proposition 1 follows similar steps as in [8, Lemma 2], and hence is omitted. \square

2) *Strongest LoS policy (SP)*: For the second pre-selection policy, we consider the case where the set of cooperative RBSs consists of the η RBSs that receive the strongest reflected signal power; see Fig. 1b. Along with the information associated to the RBSs' locations, the SP policy also requires the instantaneous channel state information of the links between the RBSs and the typical target. Similarly as before, this can be obtained through a low-rate feedback channel [5]. Then, the set of cooperative RBSs for this policy, is defined as

$$\mathcal{C}_{SP} = \left\{ u_i : u_i = \arg \max_{x \in \Phi_r \setminus \{u_1, \dots, u_{i-1}\}} \frac{h_x}{\|x\|^{2a}}, i \in \{1, \dots, \eta\} \right\}, \quad (4)$$

where h_x is the power of the channel fading between the RBS at x and the typical target. Let $\Psi = \{\|x\|^{2a}/h_x, x \in \Phi_r\}$ denotes the signal strength between each RBS at $x \in \Phi_r$ and the typical target. Without loss of generality, suppose that the elements of Ψ are indexed in an increasing order, such that $\psi_1 \leq \psi_2 \leq \dots$, where $\psi_i = \|x_i\|^{2a}/h_{x_i}$ represents the reflected signal power received by the i -th strongest LoS RBS. Since the typical target associates with the η RBSs that provide the strongest reflected signal power, then $\psi = \{\psi_1, \dots, \psi_\eta\}$ represents the reflected signal powers of the η pre-selected RBSs. The following proposition provides the cumulative distribution function (cdf) of the distance between the typical target and the strongest LoS RBS, which will be used for the detection performance when the SP policy is employed.

Proposition 2. *The cdf of the distance between the typical target and its strongest LoS RBS, is given by*

$$F_\Psi^{\text{SP}}(\psi) = \exp\left(-\pi\lambda_r \frac{\Gamma[m + \frac{1}{a}]}{m^{\frac{1}{a}} \Gamma[m]} p_L \psi^{\frac{1}{a}}\right) \mathbb{1}(\psi \leq R^{2a}). \quad (5)$$

Proof. Using the transformation $r = (h\psi)^{\frac{1}{2a}}$ and the mapping theorem [8], the intensity measure for the LoS RBSs is given by $\Lambda^{\text{SP}}(\psi) = \mathbb{E}_h \left[\pi\lambda_r p_L \psi^{\frac{1}{a}} h^{\frac{1}{a}} \right]$. The cdf of the distance between the typical target and its strongest LoS RBSs, can be computed as the probability of not having any point of the process Ψ in the interval $[0, \psi]$, i.e. $F_\Psi^{\text{SP}}(r) = \exp(-\Lambda^{\text{SP}}(\psi))$ [8]. \square

3) *Random policy (RP):* As a third pre-selection policy, we consider the case where the set of cooperative RBSs, consists of η randomly selected LoS RBSs that are located inside the LoS area. The RP policy does not require any feedback and it corresponds to a low implementation complexity. The set of cooperative RBSs is defined as

$$\mathcal{C}_{\text{RP}} = \{u_i : r_{u_i} \leq \mathfrak{R}, u_i \in \Phi_r, i \in \{1, \dots, \eta\}\}. \quad (6)$$

The following proposition provides the joint pdf of the distances between the typical target and η random LoS RBSs.

Proposition 3. *The joint pdf of the distances between the typical target and its η randomly selected LoS RBSs, is*

$$f_{\Phi_r}^{\text{RP}}(\mathbf{r}_u) = (2/R^2)^\eta \prod_{i=1}^\eta p(r_{u_i}) r_{u_i}. \quad (7)$$

Proof. The proof of Proposition 3 is similar to the proofs of the previous propositions and is omitted for brevity. \square

B. Hard Decision rules

At the second-level phase, each cooperative RBS takes an independent binary decision on the presence of the typical target. Let \mathcal{H}_0 and \mathcal{H}_1 represent the hypotheses made by each cooperative RBS, when it senses the absence and the presence of the typical target, respectively. In particular, each cooperative RBS at $u_i \in \mathcal{C}_\Pi$, where $i \in \{1, \dots, \eta\}$ and $\Pi = \{\text{CP}, \text{SP}, \text{RP}\}$, selects the hypothesis \mathcal{H}_1 , when $S_r + \mathcal{I}_r \geq \vartheta$; otherwise, it selects the hypothesis \mathcal{H}_0 . Hence, the binary decision of the cooperative RBS at $u_i \in \mathcal{C}_\Pi$, is defined as $\delta_i = 0$ if the hypothesis \mathcal{H}_0 holds, otherwise $\delta_i = 1$.

Thereafter, all local sensing informations from the cooperative RBSs are shared to the FC via an ideal report channel. In order to enhance the overall detection capability of

the considered network deployment, the FC makes the final decision by combining all local sensing informations based on an adopted fusion rule. Specifically, the FC makes the final decision according to the number of RBSs claiming the presence of their associated target. Assuming a generic κ -out-of- η fusion rule, if κ or more cooperative RBSs decides the hypothesis \mathcal{H}_1 , then the FC decides that the typical target is present. It is important to mention here that, if $\kappa = \lceil \frac{\eta}{2} \rceil$, the rule is referred as *Majority rule*, if $\kappa = 1$, the rule is referred as *OR rule*, and if $\kappa = \eta$, the rule is referred as *AND rule*.

IV. DETECTION PERFORMANCE

In this section, we analyze the impact of our proposed technique on the detection performance of RadCom systems under a constant false alarm (CFA) constraint. Initially, we derive the cdf of the power caused by the strongest interferer and the detection threshold is evaluated aiming at the achievement of the desired probability of false alarm P_{fa} . Finally, we analytically derive the detection performance achieved with the employment of our proposed technique, based on both the adopted pre-selection policies and the combining rules.

In the considered CFA operating mode, the detection threshold is selected based on a fixed target probability of false alarm P_{fa} . In order to derive compact and insightful expressions for the detection performance, the detection threshold is selected solely based on the power of the strongest interfering device [4]. The aforementioned assumption provides an approximation of the actual network's detection performance, which is shown to be tight from numerical results in Section V. Hence, we assume that the required false alarm rate, is equal to $P_{\text{fa}} = \alpha \mathbb{P}[\tilde{\mathcal{I}}_r > \vartheta]$, where $\tilde{\mathcal{I}}_r$ represents the power of the strongest device that causes interference to the serving RBS at u . The constant α is the probability that the strongest interferer is active at least once during the $M - 1$ time-slots that radar waits for the echo, and is equal to $\varrho(1 - \frac{1}{M}) + (1 - \varrho)$ [4]. In the following lemma, the cdf of $\tilde{\mathcal{I}}_r$ is analytically evaluated.

Lemma 2. *Let $\omega = P_t G^2 \ell$. The cdf of $\tilde{\mathcal{I}}$ is given by $F_{\tilde{\mathcal{I}}}(s) = \exp\left(-\frac{\lambda \phi p_L}{2} \mathcal{Y} \left(\frac{\omega}{ms}\right)^{\frac{2}{a}}\right)$, where $\mathcal{Y} = \Gamma[m + \frac{2}{a}]/\Gamma[m]$.*

Proof. See Appendix A. \square

Leveraging the expressions derived in Lemma 2, the detection threshold needed for achieving the desired false alarm rate is analytically computed in the following lemma.

Lemma 3. *The detection threshold ϑ , which ensures a false alarm rate P_{fa} , is equal to*

$$\vartheta = \frac{\omega}{m} \left(-\frac{\lambda_r \phi p_{\text{LoS}} \mathcal{Y}}{2 \ln(1 - \frac{P_{\text{fa}}}{\alpha})} \right)^{\frac{a}{2}}, \quad (9)$$

where $\omega = P_t G^2 \ell$ and $\mathcal{Y} = \Gamma[m + \frac{2}{a}]/\Gamma[m]$.

Proof. The expression is derived by replacing the expression derived in Lemma 2 in $P_{\text{fa}} = \alpha(1 - F_{\tilde{\mathcal{I}}}(\vartheta))$, and by solving the resulting equation with respect to the detection threshold. \square

Using the generic κ -out-of- η fusion rule, the final decision, conditioned on the adopted pre-selection policy Π , is given by

$$P_{\Pi}(\vartheta, \kappa) = \begin{cases} \int_{\mathbf{r}_u} \cdots \int \sum_{j=\kappa}^{\eta} \sum_{i=1}^{\eta} \prod_{i=1}^{\eta} \left(P_{\text{fa}} + \int_0^{\vartheta} \frac{\Gamma\left[m, \frac{mr^2 a_i}{\mu(s)}\right]}{\Gamma[m]} f_{\bar{T}}(s) ds \right)^{\delta_i} \left(1 - P_{\text{fa}} - \int_0^{\vartheta} \frac{\Gamma\left[m, \frac{mr^2 a_i}{\mu(s)}\right]}{\Gamma[m]} f_{\bar{T}}(s) ds \right)^{1-\delta_i} f_{\Phi_r^{\Pi}}(\mathbf{r}_u) d\mathbf{r}_u, & \text{if } \Pi = \{\text{CP}, \text{RP}\}, \\ \sum_{j=\kappa}^{\eta} \sum_{i=1}^{\eta} \prod_{i=1}^{\eta} \left(P_{\text{fa}} + \int_0^{\vartheta} \Xi(s, i) f_{\bar{T}}(s) ds \right)^{\delta_i} \left(1 - P_{\text{fa}} - \int_0^{\vartheta} \Xi(s, i) f_{\bar{T}}(s) ds \right)^{1-\delta_i}, & \text{if } \Pi = \{\text{SP}\}, \end{cases} \quad (11)$$

$$P_{\Pi}(\vartheta, \kappa) = \sum_{j=\kappa}^{\eta} \sum_{i=1}^{\eta} \prod_{i=1}^{\eta} \left(\mathcal{P}_{\Pi}^i(\vartheta) \right)^{\delta_i} \left(1 - \mathcal{P}_{\Pi}^i(\vartheta) \right)^{1-\delta_i}, \quad (10)$$

where $\kappa \in \mathbb{N}^+$, and $\mathcal{P}_{\Pi}^i(\vartheta)$ is the detection probability of the i -th cooperative RBS, which is pre-selected based on the Π policy, where $\Pi = \{\text{CP}, \text{SP}, \text{RP}\}$. Note that, δ_i is the detection decision of the cooperative RBS at $u_i \in \mathcal{C}_{\Pi}$ for the considered combination. By using the Lemma 2 and Lemma 3, the following theorem provides the network's detection performance achieved with the implementation of our proposed technique, based on the adopted pre-selection policy.

Theorem 1. *The detection performance achieved with the CoMD technique, based on the adopted pre-selection policy, is given by (11), where $F_{\Psi}^{\text{SP}}(\cdot)$ is given by Proposition 2, $f_{\bar{T}}(s) = dF_{\bar{T}}(s)/ds$, $\Xi(s, i) = \binom{\eta}{i} (F_{\Psi}^{\text{SP}}(\mu(s)))^i (1 - F_{\Psi}^{\text{SP}}(\mu(s)))^{\eta-i}$ and $\mu(s) = \frac{\omega\sigma}{4\pi(\vartheta-s)}$.*

Proof. See Appendix B. \square

V. NUMERICAL RESULTS

The spatial density of the BSs is $\lambda = 50$ BSs/km². The fraction of BSs is $\varrho = 0.7$ and the number of time-slots is equal to $M = 10$. The Nakagami fading parameter for LoS links is set to $m = 2$, while the path-loss exponent is set to $\alpha = 3$. The parameters for the sectorized antenna model are set to $G = 10$ dB and $\phi = \frac{\pi}{3}$ for the main lobe gain and beamwidth, respectively [8]. Finally, we assume that $p_L = 0.7$, $R = 200$ m, $\sigma = 10$ dB and $f = 30$ GHz [4].

Fig. 2a illustrates the achieved detection performances of the *OR*, *Majority* and *AND* hard-decision fusion rules for the considered pre-selection policies. We can first observe that the analytical results (solid, dashed and dotted lines) provide a tight upper bound for the network performance given by the simulation results (markers); this is expected due to the approximation that only the strongest BS causes interference. Another important observation from this figure is that the SP policy achieves a significantly higher network detection performance, outperforming the other two policies. We can easily observe from the figure that, the detection performance achieved with the CP and the RP policies for both the OR and the Majority rules is approximately the same. This is due to the fact that, some of the randomly selected LoS RBSs can be the same with the closest LoS RBSs, thus achieving approximately the same performance. In contrast, the detection performance achieved with the AND rule is different, since the RP policy is not able to randomly select all closest RBSs. Finally, as it can be seen in Fig. 2a, by increasing the required false alarm rate P_{fa} , the detection performance achieved for all hard-decision fusion rules and the pre-selection policies is also increased. This can be explained by the fact that, while $P_{\text{fa}} \rightarrow 1$, the

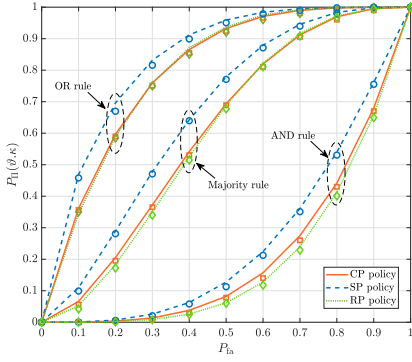
detection threshold ϑ becomes smaller, thereby increasing the number of RBSs that falsely detect the target.

Fig. 2b highlights the impact of BS cooperation on the network's detection performance, for the CP policy, compared to the conventional non-cooperative detection technique, i.e. $\eta = 1$. As expected, by increasing the number of cooperative RBSs, the detection performance achieved by applying the *OR* and the *Majority* rules increases, in contrast to the decreasing detection performance achieved by applying the *AND* rule. The latter occurs since, as the number of cooperative RBSs increases, the probability of simultaneous successful detection of a target by all cooperative RBSs is decreased. On the other hand, by applying the *OR* or the *Majority* rule, the increased number of cooperative RBSs, increases the probability of successfully detecting the target from at least one RBS or the majority of the cooperative RBSs, respectively. Fig. 2b also reveals the impact of blockages on the network's detection performance. As expected, at low LoS constant values, the existence of LoS RBSs improves the network performance, since the cooperative RBSs are able to successfully detect the target. However, by increasing the LoS constant beyond a critical point, the network performance decreases. It is important to note here that, the aforementioned conclusions also apply for the SP and the RP policies.

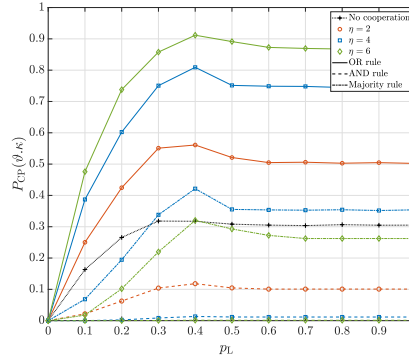
Fig. 2c illustrates the trade-off between the successful packet decode and the target detection for the CP policy versus the fraction of RBSs ϱ . We can easily observe that, for low values of ϱ , the performance of communication system increases with the fraction of RBS since the interference from nearby CBSs reduces. Beyond a critical point, the performance of the communication system is significantly reduced, since the number of CBSs and therefore the signal power received by the users decreases. Finally, the detection performance of radar systems increases with the increase of the fraction of RBSs.

VI. CONCLUSION

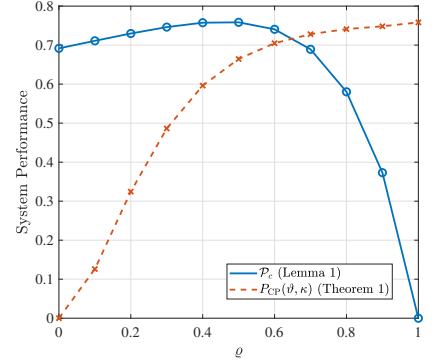
In this paper, we proposed a novel cooperative detection technique in the context of mmWave RadCom systems. Our proposed cooperation technique exploits the fusion of individual sensing decisions from the randomly deployed RBSs, aiming at enhancing the network's detection performance. We evaluated the achieved network performance in the context of several pre-selection policies and hard-decision fusion rules. Using stochastic geometry tools, the network's detection probability in the context of our proposed technique was derived in analytical derivations. Our results reveal that the SP policy outperforms in terms of achieved detection performance from the other two policies. Finally, we illustrate that the proposed technique outperforms the conventional non-cooperative detection technique. A future extension of this work is to study the



(a) Detection probability versus P_{fa} for the pre-selection policies; $\eta = 4$.



(b) Detection probability versus p_L for the CP policy; $P_{fa} = 0.3$.



(c) Communication and radar systems' performances versus ρ ; $\gamma = 0$ dB.

impact of temporal correlation on the detection performance and investigate spatially correlated RadCom systems.

APPENDIX A PROOF OF LEMMA 2

Following a reasoning similar to [8], let $\Psi_{\mathcal{I}} = \{\psi_i = \|x_i\|^a/h, x_i \in \Phi_{\mathcal{I}}\}$ denote the signal strength between each RD in $\Phi_{\mathcal{I}}$ and the cooperative RD at u_i whose elements are ordered, i.e. $\psi_i < \psi_j, \forall i < j$. Hence, based on the mapping theorem [8], the intensity measure of the PPP $\Psi_{\mathcal{I}}$, is given by

$$\Lambda((0, r]) = \frac{\lambda \phi p_L}{2} \frac{\Gamma[m + \frac{2}{a}]}{m^{\frac{2}{a}} \Gamma[m]} r^{\frac{2}{a}}, \quad (12)$$

since h is a random variable that follows Gamma distribution and by using [9, 3.381.3]. We indicate as $\tilde{x} \in \Psi_{\mathcal{I}}$, the coordinates of the strongest interferer for the cooperative RD at u_i . Hence, by denoting $\omega = p_t G^2 \ell$, the cdf of $\tilde{\mathcal{I}}$ is given by

$$F_{\tilde{\mathcal{I}}}(\theta) = \mathbb{P}[\omega h \|\tilde{x}\|^{-a} \leq \theta] = \mathbb{P}[\|\tilde{x}\|^a h^{-1} \geq \omega \theta^{-1}]. \quad (13)$$

Bearing in mind that $\|\tilde{x}\|^a/h = \psi_1$, $F_{\tilde{\mathcal{I}}}(\theta)$ can be evaluated as the probability of not having any point of the process $\Psi_{\mathcal{I}}$ in the interval $[0, \omega/\theta]$, i.e. $F_{\tilde{\mathcal{I}}}(\theta) = \exp(-\Lambda((0, \omega/\theta)))$.

APPENDIX B PROOF OF THEOREM 1

The detection probability conditioned on the RD's location, can be computed as $P_{\Pi}^i(\vartheta|r_{u_i}) = \mathbb{E}_{\mathcal{I}_{\tau}}[\mathbb{P}[\mathcal{S}_r + \mathcal{I}_{\tau} > \vartheta|\mathcal{I}_{\tau}]]$, where the interference can be either greater than the detection threshold ϑ , which marks the typical target as present regardless of the reflected signal power \mathcal{S}_r , triggering a false alarm, or less than the threshold. Hence, based on the power levels of the interference, the detection probability can be re-written as

$$P_{\Pi}^i(\vartheta|r_{u_i}) = P_{fa} + \mathbb{E}_{\mathcal{I}_{\tau}}[\mathbb{P}[\mathcal{S}_r + \mathcal{I}_{\tau} > \vartheta|\mathcal{I}_{\tau} \leq \vartheta]]. \quad (14)$$

Initially, for both the CP and the RP policies, the network's detection probability can be expressed as

$$P_{\Pi}^i(\vartheta|r_{u_i}) \stackrel{(a)}{=} P_{fa} + \mathbb{E}_{\mathcal{I}_{\tau}}\left[\Gamma\left[m, \frac{4\pi m r_{u_i}^{2a}}{\omega \sigma}(\vartheta - \mathcal{I}_{\tau})\right] / \Gamma[m]\right],$$

where (a) is derived from the fact that h_{u_i} is a random variable that follows Gamma distribution. Hence, by unconditioning the derived expressions with the distribution $f_{\tilde{\mathcal{I}}}(s) = dF_{\tilde{\mathcal{I}}}(s)/ds$, the conditional detection performance, when the CP or the RP policy is employed, is given by

$$P_{\Pi}^i(\vartheta|r_{u_i}) = P_{fa} + \int_0^{\vartheta} \Gamma\left[m, \frac{4\pi m r_{u_i}^{2a}}{\omega \sigma}(\vartheta - s)\right] f_{\tilde{\mathcal{I}}}(s) / \Gamma[m] ds.$$

Finally, by substituting the above expression into (10), and by un-conditioning with the joint pdf $f_{\Phi_{\tau}}^{\Pi}(\mathbf{r}_u)$, according to the adopted pre-selection policy, the final expression for the CP and the RP policy is derived. On the other hand, for the SP policy, based on order statistics [10] and applying the transformation $r_{u_i} = (\psi_i h_{u_i})^{\frac{1}{2a}}$, the detection probability of the i -th strongest LoS RD can be re-written as

$$P_{\Pi}^i(\vartheta) \stackrel{(a)}{=} P_{fa} + \mathbb{E}_{\mathcal{I}_{\tau}}\left[\binom{\eta}{i} \left(F_{\Psi}^{\text{SP}}(\mu(\mathcal{I}_{\tau}))\right)^i \left(1 - F_{\Psi}^{\text{SP}}(\mu(\mathcal{I}_{\tau}))\right)^{\eta-i}\right],$$

where $\mu(\mathcal{I}) = \frac{\omega \sigma}{4\pi(\vartheta - \mathcal{I}_{\tau})}$. Hence, by un-conditioning the derived expressions with the distribution $f_{\tilde{\mathcal{I}}}(s) = dF_{\tilde{\mathcal{I}}}(s)/ds$, and by substituting the resulting expression into (10), the final expression for the SP policy is derived.

REFERENCES

- [1] P. Kumari, J. Choi, N. Gonzalez-Prelcic, and R. W. Heath, Jr., "IEEE 802.11ad-based radar: An approach to joint vehicular communication-radar system," *IEEE Trans. Veh. Technol.*, vol. 67, no. 4, pp. 3012–3027, Apr. 2018.
- [2] L. Zheng, M. Lops, X. Wang, and E. Grossi, "Joint design of overlaid communication systems and pulsed radars," *IEEE Trans. Sig. Process.*, vol. 66, no. 1, pp. 139–154, Jan. 2018.
- [3] P. Ren, A. Munari, and M. Petrova, "Performance tradeoffs of joint radar-communication networks," *IEEE Wireless Commun. Lett.*, vol. 8, no. 1, pp. 165–168, Feb. 2019.
- [4] A. Munari, N. Grosheva, L. Simi, and M. Petrova, "Performance of radar and communication networks coexisting in shared spectrum bands," *arXiv preprint arXiv:1902.01359*, 2019.
- [5] C. Skouroumounis, C. Psomas, and I. Krikidis, "Low-complexity base station selection scheme in mmWave cellular networks," *IEEE Trans. Commun.*, vol. 65, pp. 4049–4064, Sept. 2017.
- [6] A. Al-Hourani, R. J. Evans, S. Kandeepan, B. Moran, and H. Eltom, "Stochastic geometry methods for modeling automotive radar interference," *IEEE Trans. Intelligent Transportation Systems*, vol. 19, no. 2, pp. 333–344, Feb. 2018.
- [7] J. Park and R. W. Heath, "Analysis of blockage sensing by radars in random cellular networks," *IEEE Signal Processing Lett.*, vol. 25, no. 11, pp. 1620–1624, Nov. 2018.
- [8] J. G. Andrews, T. Bai, M. Kulkarni, A. Alkhatieb, A. Gupta, and R. W. Heath, "Modeling and analyzing millimeter wave cellular systems," *IEEE Trans. Commun.*, vol. 65, pp. 403–430, Jan. 2017.
- [9] I. S. Gradshteyn and I. M. Ryzhik, *Table of integrals, series, and products*, in Elsevier, Academic Press, 2007.
- [10] H. C. Yang and M. S. Alouini, *Order Statistics in Wireless Communications Diversity, Adaptation, Scheduling in MIMO and OFDM Systems*, in Cambridge, U.K.: Cambridge Univ. Press, 2011.